REPORT OF SCI. AND ENG. RES. LAB., WASEDA UNIVERSITY
NO.78-5, SEPTEMBER, 1978

A Liquid Xenon Proportional Scintillation Counter

Kimiaki MASUDA, Syunsuke TAKASU, Tadayoshi DOKE,
Tan TAKAHASHI*, Atsushi NAKAMOTO**, Shinzou KUBOTA**,
Eido SHIBAMURA***

Characteristics of a liquid xenon proportional scintillation counter have been studied by using conversion electrons from ^{207}Bi. Pulse shapes of the induced charge and the scintillation in the ionization chamber mode were observed and the variations of relative photon yield of the proportional scintillation against the applied voltage were measured. Energy spectra of the proportional scintillation for ^{207}Bi were compared with those of the charge. The best resolution of the proportional scintillation was about 18 % fwhm for 1 MeV electrons, which was almost the same as that of the charge. The linear relation between the normalized photon yield at the constant electric field strength on wire surface and wire radius as expected from analogy with gas was not obtained but the tendency of increase in the normalized photon yield for wire radius was confirmed.

Science and Engineering Research Laboratory
Waseda University

* The Institute of Physical and Chemical Research

** Department of Physics, Rikkyo University

*** Saitama College of Health

1. Introduction

Occurence of electron avalanche in liquid xenon has been reported by several investigators.[1-4] In 1976, Lansiart et al.[5] found a proportional scintillation in liquid xenon, but its characteristics was not shown. Very recently, we also detected the proportional scintillation in the course of the test of a liquid xenon drift chamber using an alpha source.[6] In the experiment, the proportional scintillation pulses were used as timing signals and the spacial resolution (r.m.s.) of about 20 μm was achieved.

An energy resolution of proportional scintillation counter is determined by the ionization straggling, the fluctuation of the number of photons produced by a primary electron and the fluctuation of the number of photo-electrons in a photomultiplier. Therefore, if sufficiently large number of photons are produced and they are efficiently collected, the energy resolution of proportional scintillation counter is limited only by the ionization straggling (that is, so-called Fano factor) and is expected to be better than those of proportional counter and ionization chamber. On the basis of such consideration, gas proportional scintillation counters have been studied and have become in practical use as low energy X-ray detectors using gaseous xenon.[7-10]

Since liquid xenon has the large atomic number (Z=54), the high density (ρ=3.1 g/cm^3) and the small Fano factor ($F \approx 0.05$[11]), it is expected that liquid xenon proportional scintillation counters can be used as gamma-ray detectors with a good energy

resolution. Therefore, we have tried an experiment on energy resolution using conversion electrons from ^{207}Bi in place of alpha particles in the previous experiment.[6] Here, we report the energy resolution and relative photon yield obtained by using a liquid xenon proportional scintillation counter for different wire diameters.

2. Experimental apparatus and procedure

Fig.1 shows a schematic view of the experimental apparatus. An electrode assembly consists of a source electrode (S), a cathode of a proportional counter (K) and its center wire (W). The source electrode is a tungsten mesh of 20 mm x 30 mm with a transparency of about 85 %. ^{207}Bi source is deposited on a stainless steel plate of about 2 mm in diameter and about 100 μm in thickness placed at the center of the source electrode. The cathode is a box of the cross-section of 7.5 mm x 10 mm and the length of 30 mm without the upper face. As the center wire of the proportional counter, one of tungsten wires of 4, 6, 8.5, 10, 11 and 20 μm in diameter was strung with the tension of 80 % of the tensile strength of tungsten.

Scintillation was viewed by a photomultiplier (Hamamatsu Television R-329) through a Pyrex glass window of 8 mm thick. Sodium salicylate of about 2 mg/cm^2 thick was coated on its surface as a wavelength shifter.

A chamber vessel, a cryostat and a purification system of gaseous xenon are the same as those in ref.6. The ultimate

vacuum was 2×10^{-7} Torr and the outgassing rate was 6×10^{-8} Torr·l/sec. after baking at about 130°C for more than 50 hours.

During the experiment, the source electrode was grounded (V_S= 0 V), the cathode was kept at +4 kV (V_K= 4 kV) and the voltage higher than that of the cathode was applied to the center wire. These voltage gave the electric field of about 5-8 kV/cm between the source electrode and the cathode depending on the voltage of the center wire, V_W. In such a region of electric field strength, most of electrons are free from the recombination with ions.

Pulse shapes of charge signals obtained from the center wire were observed by a charge sensitive preamplifier which had a rise time less than 100 nsec. Pulse shapes of scintillation signals were observed at the anode of the photomultiplier with a load resistance of 50 ohm.

In the measurement of pulse heights of the charge, the outputs of the charge sensitive preamplifier were fed to a main amplifier with a pulse shaping of the differential and integral time constants of 2 μsec. On the other hand, for the proportional scintillation the signals were taken from the 6th dynode of the photomultiplier with a load resistance of 10^6 ohm and were fed to an amplifier with a pulse shaping of the differential and integral time constants of 0.5 μsec.

3. Observation of pulse shapes

Fig.2 shows typical pulse shapes of the induced charge and the scintillation in the ionization chamber mode. As seen from

Fig.2(a), firstly, the induced charge increases slowly due to the drifting of electrons from the source electrode to the center wire. Then, a rapid rise is observed. This is due to the rapid concentration of the electric field lines originated from the electron cloud to the center wire. The rise time was observed to be about 200-700 nsec. This variation depends on the range and the emission angle of electrons.

The first pulses in Fig.2(b) correspond to the direct scintillation and the following ones to the proportional scintillation. The time intervals between the both pulses correspond to the drift time of electrons and was observed to be less than 5 μsec. The time interval is not consistent with that estimated under the geometrical condition, because, from ^{207}Bi source, are emitted not only conversion electrons, but also gamma-rays which are converted at any point to electrons with high efficiency in liquid xenon.

Fig.3(a) and (b) show typical pulse shapes of the direct scintillation and the proportional scintillation, respectively. The rise time (63 % rise) of the direct scintillation was about 10 nsec and the decay time (63 % decay) was about 45 nsec. These are determined by the decay time of the sodium salicylate (8.5-10 nsec[12]) and excited molecules of xenon (27 nsec[13]). On the other hand, the pulse shape of the proportional scintillation depends very much on the range and the emission angle of electrons. The width was observed to be about 200-600 nsec, which was nearly equal to the rise time of the second part of the induced charge.

4. Energy resolution

Fig.4 shows the energy spectra for ^{207}Bi at various voltage differences between the cathode and the center wire, $V=V_W-V_K$, for the center wire of 6 μm in diameter. In the figure, the left spectra are for the proportional scintillation and the right for the charge. As seen from Fig.4, the resolution of the proportional scintillation is gradually improved as V increases and it is the best at V=3.2 kV. But the resolution becomes poor at the voltage higher than 3.2 kV. In the best spectrum of the proportional scintillation obtained at V=3.2 kV, the peak of 0.55 MeV gamma-rays and the complex peak of 0.976 MeV conversion electrons and 1.05 MeV gamma-rays are clearly seen and the resolution is about 18 % fwhm for the 1 MeV complex peak. On the other hand, the resolution of the charge does not change against the increase in V as long as the counter is used in the ionization chamber mode and it is about 16 % fwhm for the 1 MeV complex peak. But it degrades rapidly in the proportional mode. Such degradation of the energy resolution of the charge is attributed to the fluctuation in the number of electrons produced in the electron avalanche, which is caused by the roughness of the wire surface. The degradation of the energy resolution of the proportional scintillation in the higher voltage region is due to the same reason as mentioned above. Thus, the optimum voltage exists for the energy resolution of the proportional scintillation. The best resolutions for the various wire diameters were almost the same (about 16-20 % fwhm

for the 1 MeV complex peak) though the optimum voltages were different. In this experiment, the energy resolution of the proportional scintillation better than that of the charge (about 16 % fwhm for the 1 MeV complex peak) as previously expected could not be obtained.

Fig.5 shows a typical ionization spectrum and a typical proportional scintillation spectrum measured at the optimum voltage for the center wire of 11 μm in diameter, which was obtained by adjusting the gain of amplifiers so that the peaks in the both spectra may be laid at the same channel. As seen from Fig.5, the best resolution of the proportional scintillation is almost the same as that of the charge.

If the roughness of the wire surface limits the energy resolution of the proportional scintillation, the resolution must be dependent on the wire diameter. However, the results obtained in the experiment do not show such a dependency. Therefore, the limit of the resolution seems to be caused mainly by imperfect collection of electrons to the center wire. This is due to the fact that the size of the counter used in the experiment is small compared with that necessary for the perfect charge collection to the center wire when the range of electrons (about 3 mm in liquid xenon for 1 MeV electrons) and the size of the source (about 2 mm in diameter) are taken into consideration. Furthermore, gamma-rays emitted from ^{207}Bi are converted to electrons at any point. In order to overcome the former difficulty and achieve the resolution of the proportional scintillation better than that of the charge, we are constructing a new apparatus with a large proportional counter.

5. Relative photon yield in proportional scintillation

Fig.6(a),(b) and (c) show the variations of the charge gain Q, relative photon yield in the proportional scintillation L and photon yield per unit charge L/Q, respectively, versus the voltage difference V for the 1 MeV peak of ^{207}Bi for several center wires with different diameters. In Fig.6(a), the plateaus correspond to the saturation value of the ionization chamber mode and the increases of the charge gain at higher voltage mean the beginning of the electron avalanche. The electron avalanche begins at $V \approx 1.5$ kV for the center wire of 4 μm in diameter and at $V \approx 5$ kV for the center wire of 20 μm in diameter.

As seen from Fig.6(b), we could not practically observe the proportional scintillation below a certain voltage depending on the wire diameter. This fact shows the existence of a threshold electric field strength for production of photons. As shown in Fig.6(a) and (b), L increases with increasing V, while Q remains almost constant. As the electron avalanche occurs, the rate of increase in L becomes large. For the wire of 4 μm in diameter, however, L/Q decreases when the charge gain is more than about 3, as seen from Fig.6(a) and (c). For the wires of the larger diameters, only the increasing rate in L/Q decreases. These phenomena are similar to those of the gas proportional scintillation.[8)]

Recently, Conde et al.[14)] found the linear relation between the light output of the proportional scintillation and the

electric field strength by using a parallel plate gas proportional scintillation counter filled with gaseous xenon and gave an empirical equation

$$\frac{1}{p}\frac{dn}{dr} = -a + b\frac{E}{p} \quad \text{(photons/electron)cm}^{-1}\,\text{Torr}^{-1}, \quad (1)$$

where $a = 0.0074$ and $b = 0.0066$, dn/dr is the number of photons produced by an initial electron per cm, E the electric field strength (V/cm) and p the pressure of gaseous xenon (Torr). The threshold field strength for production of photons in the proportional scintillation is obtained as $E_{th} = ap/b$.

Here, we assume that such a linear relation is also applied to liquid xenon and to a cylindrical geometry. So, eq.(1) is transformed (see appendix A) into

$$n = apr_1 + \frac{bV}{\ln(r_2/r_1)}\left\{\ln\frac{bV}{apr_1\ln(r_2/r_1)} - 1\right\}, \quad (2)$$

where n is the integrated number of emitted photons, r_1 and r_2 the radii of a center wire and a cathode of the cylindrical proportional counter, respectively, and V the voltage difference between the center wire and the cathode. And relative photon yield L is written as

$$L = \eta\cdot n = B\cdot\left[Ar_1 + \frac{V}{\ln(r_2/r_1)}\left\{\ln\frac{V}{Ar_1\ln(r_2/r_1)} - 1\right\}\right], \quad (3)$$

where $A = ap/b = E_{th}$, $B = \eta\cdot b$ and η is a proportional constant. By using the electric field strength on the surface of the center wire $E_S = V/\{r_1\ln(r_2/r_1)\}$, eq.(3) is written as

$$L = Br_1\left\{A + E_S(\ln\frac{E_S}{A} - 1)\right\} \quad (4)$$

The proportional counter used in the experiment was regarded

as a cylindrical counter (see appendix B) and eq.(4) was fitted to the data of Fig.6(b) in the region of the ionization chamber mode by adjusting the parameters A (= E_{th}) and B for each run. An uncertainty of ± 10 % was assigned to each datum point. The examples of the results of the fit are shown in Fig.7 for the center wires of 4 μm, 10 μm and 20 μm in diameter. The agreement is very good for the wires of 4 μm and 10 μm in diameter, but is not so good for the wire of 20 μm in diameter. The best-fit χ^2, degrees of freedom and the best-fit values of E_{th} are given in table 1. As seen from the table, the value of E_{th} lies in the region of 4.1 - 7.0 x 10^5 V/cm. It is considered that such a variation of the value of E_{th} will be caused by the difference between the actual geometry in the experiment and the geometry used in the calculation of potential distribution and by uncertainties of wire radii. Nevertheless, it is sure that these values of E_{th} are comparable to the value 4.5 x 10^5 V/cm calculated by considering liquid xenon as gaseous xenon of 520 atm.

Moreover, from eq.(4), relative photon yield L divided by B is expected to be proportional to the wire radius when E_S is fixed. Our experimental value of relative photon yield L divided by the best-fit value of parameter B against the wire radius is plotted in Fig.8. In this figure, an uncertainty of ± 0.25 μm is allowed for each wire radius. As seen from Fig.8, a linear relation was not obtained, but the tendency of the increase in L/B at the same E_S against the wire radius was confirmed. It is considered that the difference of the experimental data from the linear relation will be due to the

same reasons as the variation of the value of E_{th}.

6. Conclusions

In the liquid xenon proportional scintillation counter, the increase in relative photon yield for the applied voltage was obtained for the wires of various diameters. This increase is approximately explained by the linear relation between the photon yield and the electric field strength in liquid xenon as well as in gaseous xenon. The threshold field strength for production of photons in liquid xenon obtained in the experiment was nearly equal to the value calculated by considering liquid xenon as gaseous xenon of 520 atm. The linear relation between the normalized photon yield at the constant electric field strength on wire surface and wire radius as expected from analogy with gas was not obtained but the tendency of increase in the normalized photon yield for wire radius was confirmed.

The energy spectra of the proportional scintillation for ^{207}Bi were compared with those of the charge in the ionization chamber mode. The energy resolution of the proportional scintillation was almost the same as that of the charge. However, it is expected that the better energy resolution will be achieved if a large counter is used. Furthermore, since we have to obtain as many photons as possible in order to achieve the good energy resolution without the electron avalanche, use of a center wire with a large diameter is recommended. This is also proper from the viewpoint that the surface of a thick wire

is considered to be more homogenious than that of a thin wire.

Appendix

A. Derivation of eq.(2)

The electric field strength in a coaxial cylinder with inner radius r_1 and outer radius r_2 is expressed by the equation

$$E = \frac{V}{r \cdot \ln(r_2/r_1)} ,$$

where E is the electric field strength, V the voltage difference between the inner and outer cylinders and r the distance from the central axis of the cylinder. Substituting the above relation into eq.(1), the following equation is obtained,

$$\frac{dn}{dr} = - ap + \frac{bV}{r \cdot \ln(r_2/r_1)} .$$

Since the proportional scintillation occurs in the region from $r = r_1$ to r_{th}, the number of emitted photons is given by integrating the above equation by r. Thus, eq.(2) is obtained as the following:

$$n = \int_{r_1}^{r_{th}} \left(-ap + \frac{bV}{r \cdot \ln(r_2/r_1)} \right) dr$$

$$= apr_1 + \frac{bV}{\ln(r_2/r_1)} \left\{ \ln \frac{bV}{apr_1 \ln(r_2/r_1)} - 1 \right\} ,$$

where

$$r_{th} = \frac{V}{E_{th} \ln(r_2/r_1)} = \frac{bV}{ap \cdot \ln(r_2/r_1)} .$$

B. Calculation of E_S

Firstly, we calculated the two-dimensional potential distributions for the geometries nearly equal to that used in the experiment (see Fig.1) by using the finite-difference approximation with an ordered relaxation method.[15] The calculations were carried out with a step (interval between calculated points) of 100 μm for the wire diameters of 4 - 20 μm and various wire potentials. The results showed that the equipotential lines near the wire is approximately circular. The deviation was about 5 % at the point of $r \sim 500$ μm, where r is the distance from the center of the wire.

Thus, we can assume a cylindrical geometry near the wire surface. Then, using the potential V(r) obtained from the above calculation for the point lying in the region of $r \sim 500$ μm, one can calculate the electric field strength at the surface of the wire, E_S, for the wire radius r_1 and the wire potential V_W, as the following:

$$E_S = \frac{V_W - V(r)}{r_1 \cdot \ln(r/r_1)} \cdot$$

References

1) R.A.Muller, S.E.Derenzo, G.Smadja, D.B.Smith, R.G.Smits, H.Zaklad and L.W.Alvarez, Phys. Rev. Letters 27 532 (1971).

2) S.E.Derenzo, T.S.Mast, H.Zaklad and R.A.Muller, Phys. Rev. A9 2582 (1974).

3) J.Prunier, R.Allemand, M.Laval and G.Thomas, Nucl. Instr. Meth. 109 257 (1973).

4) M.Miyajima, K.Masuda, A.Hitachi, T.Doke, T.Takahashi, S.Konno, T.Hamada, S.Kubota, A.Nakamoto and E.Shibamura, Nucl. Instr. Meth. 134 403 (1976).

5) A.Lansiart, A.Seigneur, J.Moretti and J.Morucci, Nucl. Instr. Meth. 135 47 (1976).

6) M.Miyajima, K.Masuda, Y.Hoshi, T.Doke, T.Takahashi, T.Hamada, S.Kubota, A.Nakamoto and E.Shibamura, Nucl. Instr. Meth. to be published.

7) C.A.Conde and A.J.P.L.Policarpo, Nucl. Instr. Meth. 53 7 (1967).

8) A.J.P.L.Policarpo, M.A.F.Alves, M.C.M.dos Santos and M.J.T. Carvalho, Nucl. Instr. Meth. 102 337 (1972).

9) D.F.Anderson, O.H.Bodine, R.Novick and R.S.Wolff, Nucl. Inst. Meth. 144 485 (1977).

10) R.D.Andresen, E.A.Leimann, A.Peacock and B.G.Taylor, Nucl. Inst. Meth. 146 391 (1977).

11) T.Doke, A.Hitachi, S.Kubota, A.Nakamoto and T.Takahashi, Nucl. Instr. Meth. 134 353 (1976).

12) G.K.Herb and W.J.Van Sciver, Rev. Sci. Instr. 36 1650 (1965).

13) S.Kubota, M.Hishida and J.Raun, J. Phys. C11 2645 (1978).

14) C.A.N.Conde, L.R.Ferreira and M.F.A.Ferreira, IEEE Trans. Nucl. Sci. NS-24 221 (1977).

15) K.M.Urbanczyk and M.P.R.Waligorski, Nucl. Instr. Meth. 124 413 (1975).

Figure Captions

Fig.1 Schematic cross-section of a liquid xenon proportional scintillation counter. S:source electrode(mesh), K: cathode of a proportional counter, W:center wire, w.l.s.: wavelength shifter. During the experiment, S was grounded, K was kept at +4 kV and the voltage higher than +4 kV was applied to W. The size of electrodes is given in mm.

Fig.2 Oscilloscope photograph of the charge and the scintillation pulses. The time scale is 1 μsec/div.
(a) Output signals at the charge sensitive preamplifier. These were triggered by direct scintillation signals.
(b) Output signals at the anode of the photomultiplier. The first signals (trigger signals) correspond to the direct scintillation and the following ones to the proportional scintillation.

Fig.3 Oscilloscope photographs of the scintillation signals at the anode of the photomultiplier.
(a) Typical direct scintillation signal. The time scale is 50 nsec/div.
(b) Typical proportional scintillation signal. The time scale is 100 nsec/div.

Fig.4 Energy spectra of ^{207}Bi for the center wire of 6 μm in diameter at various V ($V = V_W - V_K$). The left spectra

are for the proportional scintillation and the right for the charge.

Fig.5 Energy spectra of ^{207}Bi for the center wire of 11 μm in diameter at V = 4.0 kV which is the optimum voltage for this wire. The upper spectrum is for the charge and the lower for the proportional scintillation. The peak positions in both spectra are laid at the same channel.

Fig.6 (a) charge gain Q for center wires of different diameters against V ($V = V_W - V_k$). The unit gain is equal to the saturated pulse height in the ionizaion chamber mode.

(b) Relative photon yield of proportional scintillation L against V.

(c) Photon yield per unit charge L/Q against V.

Fig.7 Relative photon yield of proportional scintillation L and charge gain Q against V. Solid lines represent the results of the fit of eq.(4) to the data points in the region of the ionization chamber mode.

(a) For the wire of 4 μm in diameter. (b) For 10 μm.

(c) For 20 μm.

Fig.8 Relative photon yield L divided the best-fit value of the parameter B at $E_S = 8 \times 10^5$ V/cm against the wire radius. An uncertainty of ± 0.25 μm is allowed for each wire radius.

Table 1. The results obtained by fitting eq.(4) to the data of Fig.6(b) in the ionization chamber mode. d is the wire diameter and f is degree of freedom in the fit. The best-fit χ^2 and the best-fit value of E_{th} are given.

d	χ^2	f	E_{th}
4 μm	0.592	4	7.0×10^5 V/cm
10 μm	0.662	7	4.9×10^5 V/cm
20 μm	17.8	13	4.1×10^5 V/cm

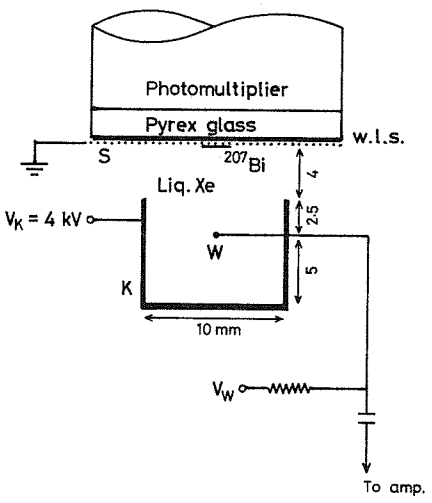

Fig. 1

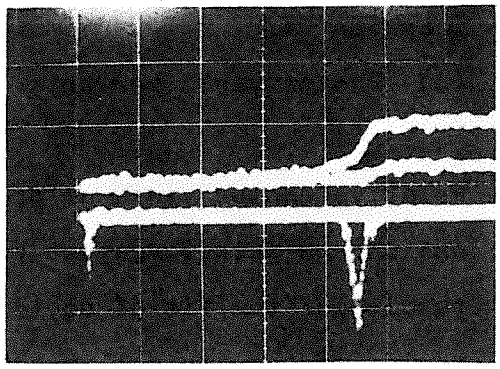

Fig. 2

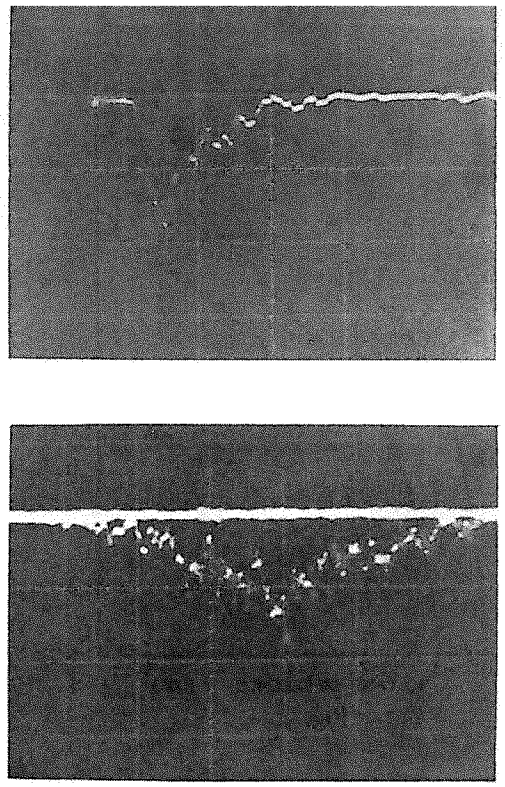

Fig. 3

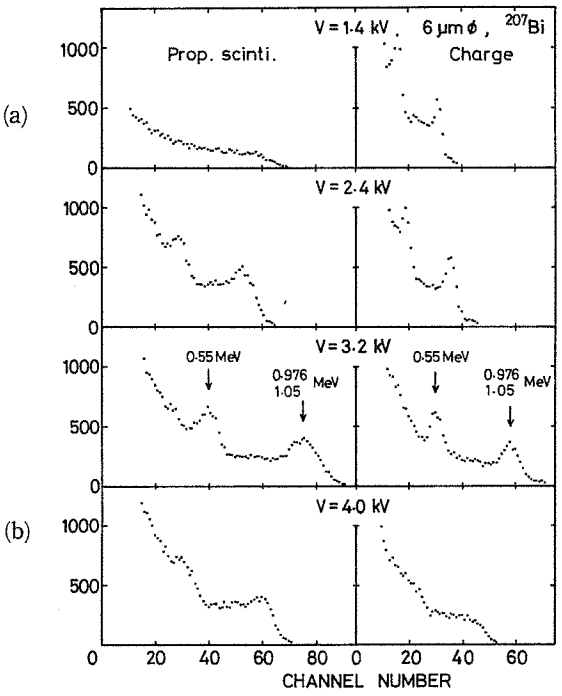

Fig. 4

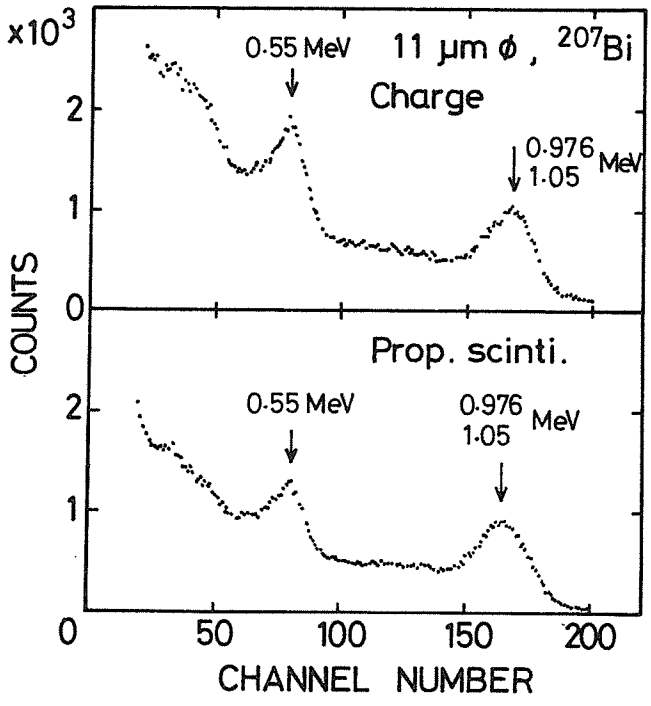

Fig. 5

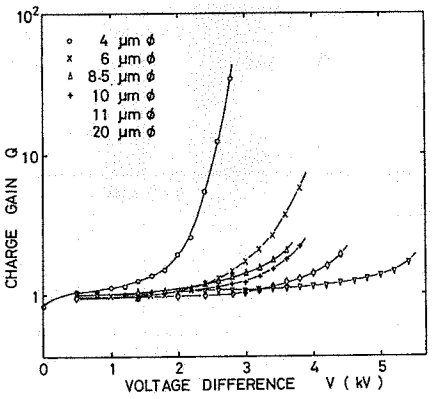

Fig. 6 (a)

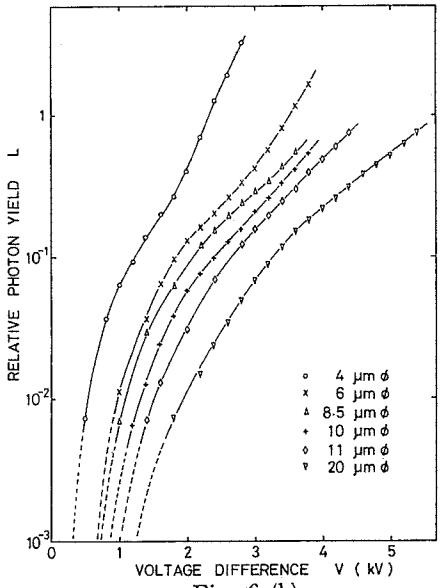

Fig. 6 (b)

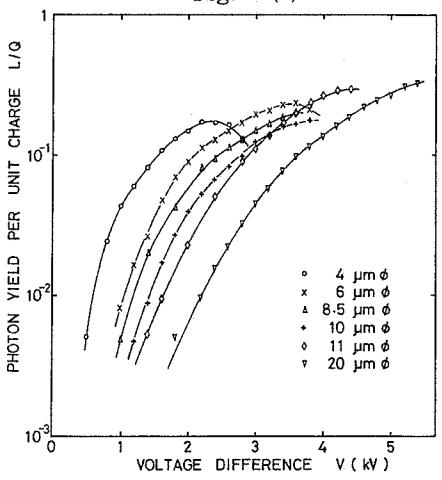

Fig. 6 (c)

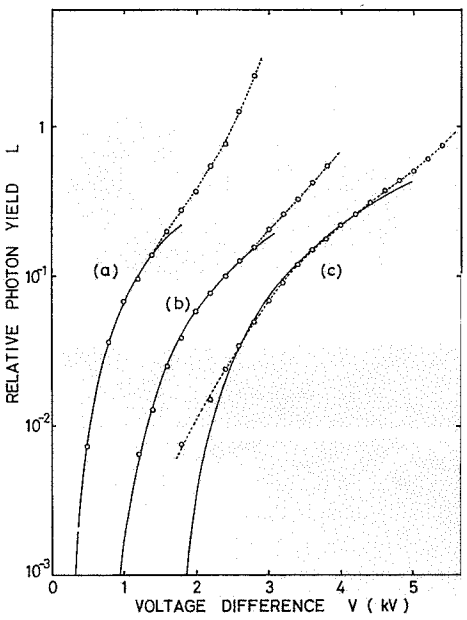

Fig. 7

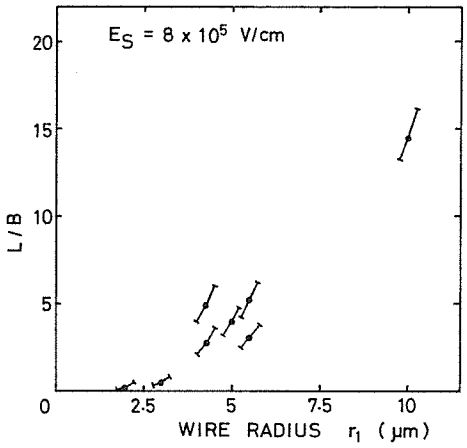

Fig. 8